



## Author Manuscript

**Title:** Carbon Nanosheets by Morphology-Retained Carbonization of Two-Dimensional Assembled Anisotropic Carbon Nanorings

**Authors:** Taizo Mori; Hiroyuki Tanaka; Amit Dalui; Nobuhiko Mitoma; Kengo Suzuki; Mutsuyoshi Matsumoto; Nikhil Aggarwal; Archita Patnaik; Somobrata Acharya; Lok Kumar Shrestha; Hirotoshi Sakamoto; Kenichiro Itami, Prof. Dr.; Katsuhiko Ariga

This is the author manuscript accepted for publication and has undergone full peer review but has not been through the copyediting, typesetting, pagination and proofreading process, which may lead to differences between this version and the Version of Record.

**To be cited as:** 10.1002/anie.201803859

**Link to VoR:** <https://doi.org/10.1002/anie.201803859>

# Carbon Nanosheets by Morphology-Retained Carbonization of Two-Dimensional Assembled Anisotropic Carbon Nanorings

Taizo Mori,<sup>[a,†]</sup> Hiroyuki Tanaka,<sup>[b,†]</sup> Amit Dalui,<sup>[a]</sup> Nobuhiko Mitoma,<sup>[b]</sup> Kengo Suzuki,<sup>[d]</sup> Mutsuyoshi Matsumoto,<sup>[d]</sup> Nikhil Aggarwal,<sup>[e]</sup> Archita Patnaik,<sup>[e]</sup> Somobrata Acharya,<sup>[f]</sup> Lok Kumar Shrestha,<sup>[a]</sup> Hirotohi Sakamoto,<sup>[b]</sup> Kenichiro Itami,<sup>\*[b,c]</sup> and Katsuhiko Ariga<sup>\*[a,g]</sup>

**Abstract:** Two-dimensional (2D) carbon nanomaterials possessing promising physical and chemical properties find applications in high-performance energy storage devices and catalysts. However, large-scale fabrication of 2D carbon nanostructures is based on a few specific carbon templates or precursors and poses a formidable challenge. Here, we report a new bottom-up methodology for carbon nanosheet fabrication using a newly designed anisotropic carbon nanoring molecule, CPPhen. CPPhen was self-assembled at a dynamic air-water interface with a vortex motion to afford molecular nanosheets, which were then carbonized under inert gas flow. Their nanosheet morphologies were retained after carbonization, which has never been seen for low-molecular weight compounds. Furthermore, adding pyridine as a nitrogen dopant in the self-assembly step successfully afforded nitrogen-doped carbon nanosheets containing mainly pyridinic nitrogen species.

Various carbon nanomaterials obtained by bottom-up

approaches such as nanotubes,<sup>[1]</sup> nanoribbons<sup>[2–4]</sup> and nanosheets<sup>[5–12]</sup> have attracted immense interest due to versatile applications in sensing and separation and in electronic and optical devices because of their outstanding physical and chemical properties.<sup>[13–16]</sup> In particular, the fabrication of large-scale carbon nanosheets as two-dimensional (2D) functional nanomaterials with sp<sup>2</sup> carbon-rich networks has been a subject of intense research toward potential device applications. To obtain a large-scale uniform nanosheet morphology, various interfaces have been used as a self-assembly field.<sup>[17–19]</sup> While a vacuum deposition process is advantageous to obtain molecular nanomaterials with uniform morphologies at the vacuum-solid interface, solution processes are much simpler in providing nanomaterials with large-scale 2D morphologies under mild conditions. Particularly, Langmuir-Blodgett (LB)-based self-assembly at an air-water interface is suitable for controlling the compositions and orientations of nanostructures by changing surface pressures.<sup>[20,21]</sup>

Carbonization of 2D self-assembled molecular nanomaterials is an effective way to obtaining structurally well-defined carbon nanosheets.<sup>[6,7]</sup> However, this process, which involves the calcination of self-assembled  $\pi$ -conjugated small molecules at high temperature, presents a significant problem. It is difficult to retain the morphology of the original thin films made of small molecules during carbonization due to thermal decomposition and volatilization of hydrocarbon gases that destroy the original morphology, even though some  $\pi$ -conjugated polymers can be carbonized in the same condition.<sup>[22]</sup> Therefore, general strategy for the bottom-up fabrication of large-scale carbon nanosheets, which do not require a specific carbon template or precursor with specific chemical reactivity, is critically important.<sup>[2–6]</sup> Many aromatic molecules show intermolecular interactions such as alkyl-alkyl and/or C–H/ $\pi$  which we think can be utilized to retain the original morphology during calcination process. Herein, we introduce a new carbon-rich  $\pi$ -conjugated anisotropic macrocycle, 9,9',10,10'-tetrabutoxy-cyclo[6]-paraphenylene[2]-3,6-phenanthrenylene (CPPhen). The ellipsoidal CPPhen effectively afforded smooth 2D molecular films through self-assembly at a dynamic interface with a vortex motion,<sup>[23]</sup> which were subsequently subjected to a carbonization process to obtain carbon nanosheets (Figure 1). The 2D morphology was retained during the high-temperature carbonization process, which proved that the anisotropic molecule with intermolecular interaction is highly suitable as a carbonization template. Furthermore, nitrogen (N)-doped carbon nanosheets were successfully fabricated from the CPPhen-based vortex film.

[a] Dr. T. Mori, Dr. A. Dalui, Dr. L. K. Shrestha, Dr. K. Ariga  
World Premier International (WPI) Center for Materials  
Nanoarchitectonics (NAMA)  
National Institute for Materials Science (NIMS)  
Namiki 1-1, Tsukuba, Ibaraki 305-0044 (Japan)  
E-mail: [ARIGA.Katsuhiko@nims.go.jp](mailto:ARIGA.Katsuhiko@nims.go.jp)

[b] Dr. H. Tanaka, Dr. N. Mitoma, Dr. H. Sakamoto Prof. Dr. K. Itami  
JST-ERATO Itami Molecular Nanocarbon Project and Graduate  
School of Science  
Nagoya University  
Chikusa, Nagoya 464-8602 (Japan)  
E-mail: [itami@chem.nagoya-u.ac.jp](mailto:itami@chem.nagoya-u.ac.jp)

[c] Prof. Dr. K. Itami  
Institute of Transformative Bio-Molecules (WPI-ITbM)  
Nagoya University  
Chikusa, Nagoya 464-8602 (Japan)

[d] Dr. K. Suzuki, Prof. Dr. M. Matsumoto  
Department of Materials Science and Technology  
Tokyo University of Science,  
6-3-1 Niiijuku, Katsushika-ku, Tokyo 125-8585, Japan

[e] Dr. N. Aggarwal, Dr. A. Patnaik  
Department of Chemistry  
Indian Institute of Technology Madras, Chennai 600 036, India

[f] Dr. S. Acharya  
Center for Advanced Materials (CAM)  
Indian Association for the Cultivation of Science (IACS)  
Jadavpur, Kolkata 700 032 (India)

[g] Prof. Dr. K. Ariga  
Graduate School of Frontier Sciences  
The University of Tokyo, Kashiwa 277-0827, Japan

[†] These authors contributed equally.  
Supporting information for this article is available on the WWW  
under <http://>  
Crystallography data for CPPhen in CIF format (CIF)  
Additional information concerning the synthesis, crystal packing,  
thin-film fabrication, BAM, AFM, IR-RAS analysis, TGA, and Raman  
spectra (PDF)

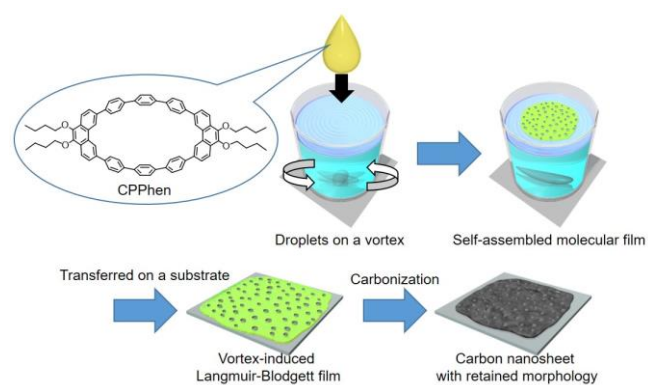


**Figure 1.** Schematic illustration of the fabrication of large-scale uniform carbon nanosheets. Chemical structure of CPPhen, illustrations of key steps in the fabrication of carbon nanosheets by the vortex LB technique (Step 1: The chloroform solution of CPPhen is placed dropwise and spread onto a water subphase with vortex motion; Step 2: After stirring was stopped, the system is left to stand to evaporate the remaining solvent to obtain a thin film on the water surface; Step 3: The film is transferred onto a substrate), and the subsequent carbonization process of the CPPhen-based thin film at high temperatures under nitrogen flow (Step 4).

CPPhen was designed to have an anisotropic molecular symmetry, which would promote an anisotropically oriented 2D molecular assembly at an air-water interface (Figure 1). The phenanthrene units in CPPhen can be expected to work as a core of a graphitization during the high-temperature carbonization process because of the higher thermal stability than those of the *p*-phenylene units.<sup>[6]</sup> The ellipsoidal macrocyclic structure is expected not to exhibit strong interactions as highly planar molecules form, such as  $\pi$ - $\pi$  stacking leading to crystalline columnar structures.<sup>[24]</sup> In addition, the *n*-butoxy side chains are expected to show strong repulsion against the water surface due to their hydrophobic character, as well as intermolecular alkyl-alkyl interactions. These structural features can be confirmed in the single-crystal X-ray structure (Supporting Information, Figure S1).

A dynamic air-water interface provides extra force to the substance on the interface, which can be utilized to control the orientation and morphology of 2D nanostructures.<sup>[25–28]</sup> Our recently developed vortex LB technique employs a dynamic air-water interface with a vortex motion induced by the flow of a centrifugal rotation.<sup>[17]</sup> To weaken the strong aggregation tendency of CPPhen and spread the molecules uniformly on the air-water interface, we attempted thin-film fabrication using the vortex LB technique (Supporting Information). When the CPPhen solution in chloroform (200  $\mu$ M; 50  $\mu$ L) was spread onto the water subphase at 25 °C under a dynamic stirring condition with 100 rpm stirring speed and 2 min stirring time, the resulting vortex LB film transferred onto a silicon substrate showed a uniform and flat nanostructure with thickness as large as 10 nm and width over several tens of micrometer (Figure 2a). In addition, the vortex LB film possessed mesopores with an average diameter of about 40 nm within the 2D uniform morphology (Figure 2b). Transmission electron microscopy (TEM) images of the directly transferred vortex LB film onto a

TEM grid revealed that the pores are extended through the film (Figure 2c).

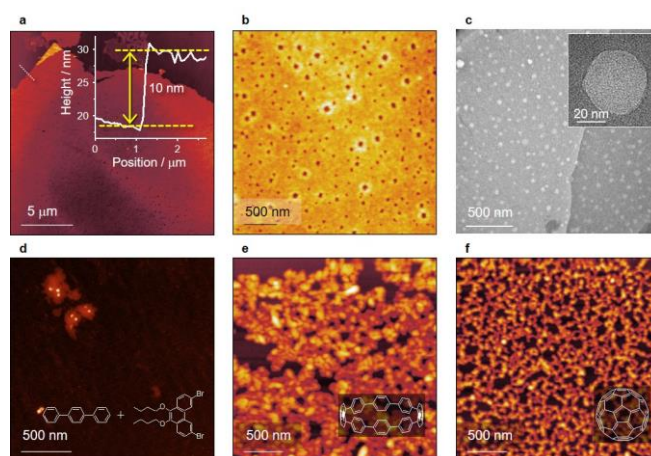


**Figure 2.** Characterization of CPPhen-based vortex LB thin films. (a) AFM image of the CPPhen-based vortex LB film on a Si substrate with a cross-section profile along the dotted line. (b) High-magnification AFM image of CPPhen film showing a mesoporous structure. (c) TEM image of the vortex LB film transferred onto a carbon-coated copper grid. The pores are seen as white dots. Inset shows a high-magnification TEM image of a single pore with diameter of about 40 nm. The carbon mesh of the TEM grid can be observed through the pores. (d–f) AFM images of the obtained objects fabricated from a mixture of *p*-terphenyl and phenanthrene derivative (d), [10]CPP (e), and  $C_{60}$  (f).

The use of CPPhen template proved important to attaining the uniform 2D morphology. When other  $\pi$ -conjugated compounds including components of CPPhen, highly symmetric carbon nanoring ([10]cycloparaphenylene, [10]CPP), and fullerene ( $C_{60}$ ) were used for the vortex LB assembly in the same condition as that of CPPhen, 2D uniform morphology was not observed (Figure 2d–f and S3 in Supporting Information). These results show that the anisotropic macrocyclic structure and alkyl chains of CPPhen effectively afford suitable intermolecular interactions to form a thin-film assembly at the vortical air-water interface.

Based on the AFM observations with additional spectroscopic and diffraction measurements (Supporting Information, Figure S4, S9 and S10), a mechanism for the vortex-induced thin film formation by the vortex LB technique can be anticipated (Supporting Information, Figure S11). The thickness of ca. 10 nm, shown in Figure 2a, indicates that five molecular layers are stacked in the tandem nanostructure. During domain aggregation, some defects are generated among the domain units, in which the solvent is trapped. Evaporation of the chloroform solvent from the defects affords mesoporous nanostructure. The macrocyclic structure of CPPhen can also serve as a cavity for solvent trapping,<sup>[29]</sup> but it is too small (sub-nanometer size) to be observed in the AFM images.

As a result, both the ellipsoidal macrocyclic structure and hydrophobic character of CPPhen fully cooperated to form the assembled domain nanostructures with almost perpendicular orientations of CPPhen to the water surface (Supporting Information, Figure S11c). The vortical air-water interface largely

contributed to the formation of a large-scale uniform thin film of CPPhen without immediate aggregation. Although a full understanding of the structure-property relationship of CPPhen-based thin film formation requires further extensive investigation, the unique anisotropic molecular conformation and orientation of CPPhen most likely led to the formation of the domain nanostructures.

The carbonization of CPPhen-based vortex LB films on Si substrates was examined by heat treatments at 850 °C for 3 h under N<sub>2</sub> gas flow, resulting in large-scale carbon nanosheets (Figure 3a). Surprisingly, the mesoporous morphology observed for the vortex LB films was retained even after the carbonization process (Figure 3c). The thicknesses of the carbonized films remained unchanged (ca. 10 nm), while the pore diameters were 20 ~ 30 nm, that is, slightly smaller than those of the pristine CPPhen-based vortex LB films. The high-resolution (HR) TEM image of the carbonized nanosheet object shows a typical turbostratic carbon structure, in which curved carbon atom layers were randomly stacked. The distance between the carbon atom layers was ca. 0.36 nm, close to the interplanar spacing of graphite (Figure 3b), which guarantees some graphitic characters for the carbon nanosheet, as observed from the enhancement in electrical conductivity (Figure 3d). The conductivity was calculated as  $1.98 \times 10^3$  S/m.

Although the morphology-retaining carbonization of  $\pi$ -conjugated polymeric materials preprocessed by iodine doping has already reported,<sup>[30]</sup> this is the first example of preparation of a uniform carbon nanosheet from the 2D molecular assembly of a low-molecular weight  $\pi$ -conjugated molecule. We surmise that this morphology retention is due to the suitable intermolecular interactions between the CPPhen molecules such as alkyl-alkyl and C-H/ $\pi$  interactions, which kept the carbonaceous constituent of CPPhen bound together in the vortex LB films even during thermal decomposition and volatilization of hydrocarbon gases. From the viewpoint of the molecular design of CPPhen, we considered that the thermally stable phenanthrene units largely contributed to the graphitization and subsequent morphology-retaining carbonization. Thus, large-scale uniform carbon nanosheets were obtained, retaining the original morphology of the vortex LB films.

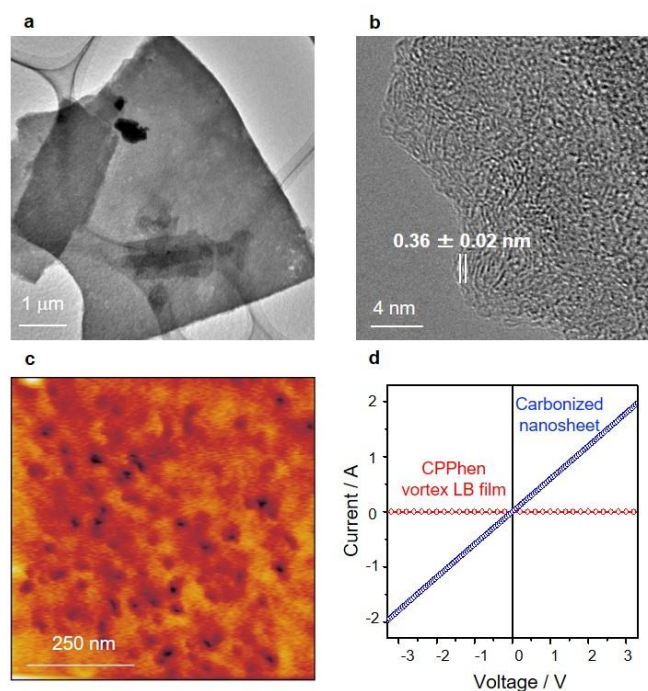


**Figure 3.** Characterization of carbon nanosheets. (a) TEM image of carbon nanosheet prepared by the carbonization of CPPhen-based vortex LB film at 850 °C for 3 h under N<sub>2</sub> gas flow. (b) HR-TEM image of carbon nanosheet exhibiting a turbostratic carbon structure with a distance of  $0.36 \pm 0.02$  nm between the carbon layers. (c) AFM image of carbon nanosheet with mesoporous structure. (d) *I-V* characteristics of CPPhen-based vortex LB film (red line) and the carbon nanosheet prepared by carbonization at 850 °C (blue line).

N-doped carbon nanosheets were easily fabricated through the vortex LB technique and the subsequent carbonization process (Figure 4, details in Supporting Information). Pyridine was used as the N dopant and mixed in the CPPhen solution for the vortex LB assembly with a molar ratio, CPPhen/pyridine = 5:1, affording a N-doped molecular nanosheet. Then the N-doped nanosheet was carbonized in the same way as that of the non-doped one. The versatility allowing facile modification is an advantage of the LB technique involving air-water interfaces.

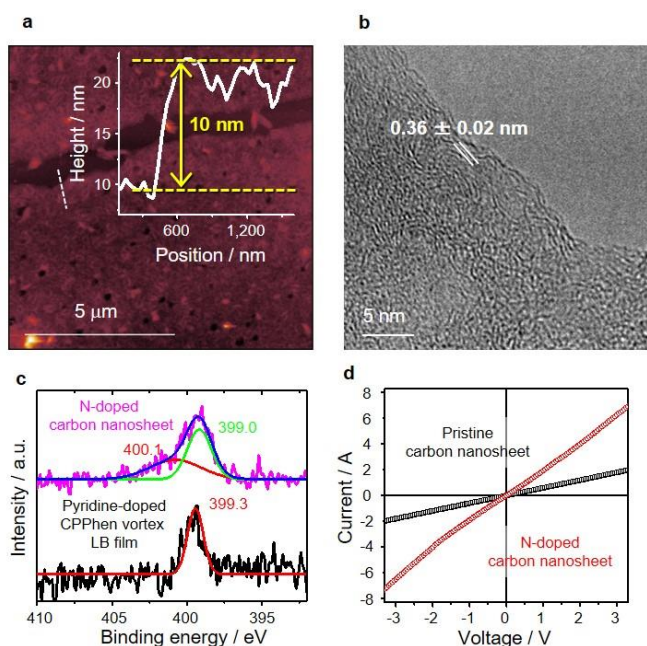


**Figure 4.** Characterization of N-doped carbon nanosheets. (a) AFM image of N-doped carbon nanosheet fabricated at 850 °C. Inset shows the cross-section profile along the white line. (b) HR-TEM image of N-doped carbon nanosheet exhibiting a distance of  $0.35 \pm 0.02$  nm between the carbon layers. (c) XPS N 1s core level spectra of CPPhen-based vortex LB film including pyridine molecules (lower) and N-doped carbon nanosheet fabricated at 850 °C (upper). The deconvoluted peaks at around 399 and 400 eV indicate the existence of both pyridinic (green line) and pyrrolic (red line) nitrogen species in the carbon nanosheet. (d)  $I$ - $V$  characteristics of carbon nanosheets with and without N-doping.

The N-doped carbon nanosheet showed uniform distributions of oxygen, carbon, and nitrogen throughout the nanosheet, revealed by TEM-energy dispersive X-ray spectrometry (TEM-EDX) elemental mapping (Supporting Information, Figure S14). Surprisingly, the nitrogen species remained in the carbonized product even after calcination at 850 °C, although the boiling point of pyridine is 116 °C. The nitrogen and oxygen contents in the N-doped carbon nanosheet were calculated to be 6.0 and 1.0%, respectively, by the corrected analysis of the EDX spectrum. X-ray photoelectron spectroscopy (XPS) measurements revealed that the nitrogen species in the N-doped carbon nanosheet were mainly pyridinic with a small fraction of pyrrolic ones, as calculated by the deconvolution of the combined nitrogen peak at around 399 eV (Figure 4c and S15 in Supporting Information). The majority of residual oxygen species indicates aromatic C-O groups (around 533 eV) after the carbonization. The remarkably high N-doping amount in the obtained carbon nanosheets (~6.0 %) can be explained by assuming that the dopant pyridine molecules are efficiently trapped into the cavity of each CPPhen macrocycle or in the interstices of the packed CPPhen molecules in the assembled tandem nanostructures, even at temperatures over its boiling point. The electrical conductivity of the N-doped carbon nanosheet ( $8.34 \times 10^3$  S/m) was better than that of the

pristine one (Figure 4d), which should originate from the effect of N doping.

In summary, we have demonstrated a new remarkably easy method for the bottom-up fabrication of large-scale uniform carbon nanosheets by 2D molecular assembly of an anisotropic macrocyclic molecule, CPPhen, at the vortical air-water interface and subsequent carbonization. Due to the properly designed intermolecular interactions of CPPhen and the extra assembling force induced by the vortex motion, uniform 2D molecular assemblies and morphology-retaining carbonization have been realized. This is the first example of 2D morphology-retaining carbonization of a molecular assembly with a low-molecular weight  $\pi$ -conjugated molecule, affording a new type of carbon nanomaterial without the aid of traditional polymeric carbon-rich precursors. We have confirmed that some other CPPhen type molecules with ellipsoidal ring structures and alkoxy chains afford smooth molecular films, exemplifying our molecular design is reasonable. Investigations of these molecular films are to be further investigated for carbonization. Easy fabrication of N-doped carbon nanosheets was realized just by adding pyridine as a dopant into the CPPhen solution and the subsequent carbonization. The amount of pyridinic nitrogen species doped in the 2D nanosheets was unexpectedly high, which would allow the utilization of N-doped carbon nanosheets as highly efficient catalysts for oxygen-reduction reactions for high-performance fuel cells.<sup>[31–34]</sup>

## Acknowledgements

This work was partially supported by the ERATO program of JST (K.I.) (grant number: JPMJER1302), JSPS KAKENHI (16H07436, JP16H06518 (Coordination Asymmetry)), and CREST (JPMJCR1665). We thank T. Matsumoto (Kyusyu University) for the single-crystal X-ray diffraction measurement and K. Oyama (Nagoya University) for mass spectrometry analyses. ITbM is supported by the World Premier International Research Center Initiative (WPI), Japan.

**ORCID:** Kenichiro Itami: 0000-0001-5227-7894

**Keywords:** Nanosheet • carbon nanoring • LB film fabrication • self-assembly • nitrogen doping

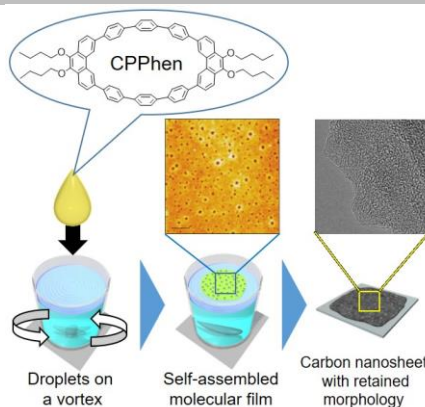
- [1] J. R. Sanchez-Valencia, T. Dienel, O. Gröning, I. Shorubalko, A. Mueller, M. Jansen, K. Amsharov, P. Ruffieux, R. Fasel, *Nature* **2014**, *512*, 61–64.
- [2] J. Cai, P. Ruffieux, R. Jaafar, M. Bieri, T. Braun, S. Blankenburg, M. Muoth, A. P. Seitsonen, M. Saleh, X. Feng, K. Müllen, R. Fasel, *Nature* **2010**, *466*, 470–473.
- [3] A. Narita, X. Feng, Y. Hernandez, S. A. Jensen, M. Bonn, H. Yang, I. A. Verzhbitskiy, C. Casiraghi, M. R. Hansen, A. H. R. Koch, G. Fytas, O. Ivasenko, B. Li, K. S. Mali, T. Balandina, S. Mahesh, S. D. Feyter, K. Müllen, *Nat. Chem.* **2014**, *6*, 126–132.
- [4] P. Ruffieux, S. Wang, B. Yang, C. Sanchez-Sanchez, J. Liu, T. Dienel, L. Talirz, P. Shinde, C. A. Pignedoli, D. Passerone, T. Dumslaff, X. Feng, K. Müllen, R. Fasel, *Nature* **2016**, *531*, 489–492.

- [5] M. Bieri, M. Treier, J. Cai, K. Ait-Mansour, P. Ruffieux, O. Gröning, P. Gröning, M. Kastler, R. Rieger, X. Feng, K. Müllen, R. Fasel, *Chem. Commun.* **2009**, 45, 6919–6921.
- [6] P. Angelova, H. Vieker, N.-E. Weber, D. Matei, O. Reimer, I. Meier, S. Kurasch, J. Biskupek, D. Lorbach, K. Wunderlich, L. Chen, A. Terfort, M. Klapper, K. Müllen, U. Kaiser, A. Götzhäuser, A. Turchanin, *ACS Nano* **2013**, 7, 6489–6497.
- [7] D. G. Matei, N.-E. Weber, S. Kurasch, S. Wundrack, M. Woszczyzna, M. Grothe, T. Weimann, F. Ahlers, R. Stosch, U. Kaiser, A. Turchanin, *Adv. Mater.* **2013**, 25, 4146–4151.
- [8] S. Schrettl, C. Stefaniu, C. Schwieger, G. Pasche, E. Oveisi, Y. Fontana, A. F. Morral, J. Reguera, R. Petraglia, C. Corminboeuf, G. Brezesinski, H. Frauenrath, *Nat. Chem.* **2014**, 6, 468–476.
- [9] C. H. A. Wonga, M. Pumera, *Phys. Chem. Chem. Phys.* **2013**, 15, 7755–7759.
- [10] A. Ambrosi, C. K. Chua, A. Bonanni, M. Pumera, *Chem. Rev.* **2014**, 114, 7150–7188.
- [11] N. Raghavana, S. Thangavela, G. Venugopal, *Appl. Mater. Today* **2017**, 7, 246–254.
- [12] A. B. Bourlino, V. Georgakilas, V. Mouselimis, A. Kouloumpis, E. Mouzourakis, A. Koutsoukis, M.-K. Antoniou, D. Gournis, M. A. Karakassides, Y. Deligiannakis, V. Urbanova, K. Cepe, A. Bakandritsos, R. Zboril, *Appl. Mater. Today* **2017**, 9, 71–76.
- [13] H. Zhang, *ACS Nano* **2015**, 9, 9451–9469.
- [14] J. Wan, S. D. Lacey, J. Dai, W. Bao, M. S. Fuhrer, L. Hu, *Chem. Soc. Rev.* **2016**, 45, 6742–6765.
- [15] C. Tan, X. Cao, X.-J. Wu, Q. He, J. Yang, X. Zhang, J. Chen, W. Zhao, S. Han, G.-H. Nam, M. Sindoro, H. Zhang, *Chem. Rev.* **2017**, 117, 6225–6331.
- [16] A. H. Khan, S. Ghosh, B. Pradhan, A. Dalui, L. K. Shrestha, S. Acharya, K. Ariga, *Bull. Chem. Soc. Jpn.* **2017**, 90, 627–648.
- [17] K. Ariga, T. Mori, J. P. Hill, *Langmuir* **2013**, 29, 8459–8471.
- [18] K. Ariga, V. Malgras, Q. Ji, M. B. Zakaria, Y. Yamauchi, *Coord. Chem. Rev.* **2016**, 320–321, 139–152.
- [19] K. Ariga, T. Mori, W. Nakanishi, J. P. Hill, *Phys. Chem. Chem. Phys.* **2017**, 19, 23658–23676.
- [20] T. Mori, K. Sakakibara, H. Endo, M. Akada, K. Okamoto, A. Shundo, M. V. Lee, Q. Ji, T. Fujisawa, K. Oka, M. Matsumoto, H. Sakai, M. Abe, J. P. Hill, K. Ariga, *Langmuir* **2013**, 29, 7239–7248.
- [21] K. Sakakibara, P. Chithra, B. Das, T. Mori, M. Akada, J. Labuta, T. Tsuruoka, S. Maji, S. Furumi, L. K. Shrestha, J. P. Hill, S. Acharya, K. Ariga, A. Ajayaghosh, *J. Am. Chem. Soc.* **2014**, 136, 8548–8551.
- [22] V. Malgras, Q. Ji, Y. Kamachi, T. Mori, F.-K. Shieh, K. C.-W. Wu, K. Ariga, Y. Yamauchi, *Bull. Chem. Soc. Jpn.* **2015**, 88, 1171–1200.
- [23] V. Krishnan, Y. Kasuya, Q. Ji, M. Sathish, L. K. Shrestha, S. Ishihara, K. Minami, H. Morita, T. Yamazaki, N. Hanagata, K. Miyazawa, S. Acharya, W. Nakanishi, J. P. Hill, K. Ariga, *ACS Appl. Mater. Interfaces* **2015**, 7, 15667–15673.
- [24] X. Feng, V. Marcon, W. Pisula, M. R. Hansen, J. Kirkpatrick, F. Grozema, D. Andrienko, K. Kremer, K. Müllen, *Nat. Mater.* **2009**, 8, 421–426.
- [25] K. Ariga, T. Mori, J. P. Hill, *Adv. Mater.* **2012**, 24, 158–176.
- [26] K. Ariga, S. Ishihara, H. Izawa, H. Xia, J. P. Hill, *Phys. Chem. Chem. Phys.* **2011**, 13, 4802–4811.
- [27] K. Ariga, T. Mori, S. Ishihara, K. Kawakami, J. P. Hill, *Chem. Mater.* **2014**, 26, 519–532.
- [28] K. Ariga, Y. Yamauchi, T. Mori, J. P. Hill, *Adv. Mater.* **2013**, 25, 6477–6512.
- [29] K. B. Burke, W. J. Belcher, L. Thomsen, B. Watts, C. R. McNeill, H. Ade, P. C. Dastoor, *Macromolecules* **2009**, 42, 3098–3103.
- [30] S. Matsushita, M. Kyotani, K. Akagi, *J. Am. Chem. Soc.* **2011**, 133, 17977–17992.
- [31] J. Diao, H. Liu, J. Wang, Z. Feng, T. Chen, C. Miao, W. Yang, D. S. Su, *Chem. Commun.* **2015**, 51, 3423–3425.
- [32] C. Tang, H.-F. Wang, X. Chen, B.-Q. Li, T.-Z. Hou, B. Zhang, Q. Zhang, M.-M. Titirici, F. Wei, *Adv. Mater.* **2016**, 28, 6845–6851.
- [33] C. Su, M. Acik, K. Takai, J. Lu, S.-J. Hao, Y. Zheng, P. Wu, Q. Bao, T. Enoki, Y. J. Chabal, K. P. Loh, *Nat. Commun.* **2012**, 3, 1298.
- [34] J. Bai, X. Zhong, S. Jiang, Y. Huang, X. Duan, *Nat. Nanotech.* **2010**, 5, 190–194.

Entry for the Table of Contents (Please choose one layout)

## COMMUNICATION

A new bottom-up methodology for carbon nanosheet fabrication using a newly designed anisotropic carbon nanoring molecule, CPPhen was developed. CPPhen was self-assembled at a dynamic air-water interface with a vortex motion to afford molecular nanosheets, which were then carbonized under inert gas flow. Their nanosheet morphologies were retained after carbonization.



Taizo Mori, Hiroyuki Tanaka, Amit Dalui, Nobuhiko Mitoma, Kengo Suzuki, Mutsuyoshi, Matsumoto, Nikhil Aggarwal, Archita Patnaik, Somabrata Acharya, Lok Kumar Shrestha, Hirotohi Sakamoto, Kenichiro Itami\*, and Katsuhiko Ariga\*

Page No. – Page No.

**Carbon Nanosheets by Morphology-Retained Carbonization of Two-Dimensional Assembled Anisotropic Carbon Nanorings**

Author Manuscript